Building Simulation 2009

Eleventh International IBPSA Conference
Glasgow, Scotland
July 27-30, 2009

A PROTOTYPE MESH GENERATION TOOL DEVELOPMENT FOR CFD SIMULATIONS IN ARCHITECTURE DOMAIN

Rui Zhang[1], Yongjie Zhang[2], Khee Poh Lam[1], David H. Archer[2]
[1]Center for Building Performance and Diagnostics, School of Architecture
[2]Department of Mechanical Engineering
Carnegie Mellon University, 15213, Pittsburgh, PA

ABSTRACT

Computational Fluid Dynamics (CFD) has been introduced to the architectural engineering and HVAC (Heating Ventilation and Air Conditioning) industry for decades. Its effectiveness in assisting the architects and engineers in the design process has been well acknowledged. However, the mesh generation process is complicated and time consuming, especially for modeling free form geometric artifacts, e.g., buildings in complex terrains or human bodies in the room. This paper presents the effort to apply quality mesh generation to CFD simulations in architectural applications.

A prototype meshing tool is developed to construct adaptive quadrilateral meshes from two-dimensional image data, e.g., architecture drawings. First the quad-tree based isocontouring method is utilized to generate initial uniform quadrilateral meshes in the immediate region surrounding the boundary of the objects. Boundary vertices are recalculated to improve the geometry accuracy. Meshes are decomposed into finer quads adaptively near the surface of the object without introducing any hanging nodes. Boundary layers are generated using the pillowing technique and the thickness of the boundary layer is controlled to achieve the desired y^+ values, according to various requirements of near wall turbulence models. After generating fine meshes in the immediate region, the meshes are extended to the ambient domain with desired sizes, where flow fields are relatively steady. The developed tool has been employed to generate meshes for two demonstrations: the wind flow field at the ambient of the Reichstag Building (high-Reynolds-number flow), and the natural convection around an occupant in the indoor environment (low-Reynolds-number flow).

KEYWORDS

Architecture, CFD, geometry, quadrilateral mesh, quadtree, pillowing, boundary layer

INTRODUCTION

Computational Fluid Dynamics (CFD) has been introduced to the architectural engineering and HVAC (Heating Ventilation and Air Conditioning) industry for decades. Its effectiveness in assisting the architects and engineers in the design process has been well acknowledged. The first step in CFD simulation is to discretize the computational domain, which is also called mesh generation. Mesh quality is critical to CFD computations. Most of the currently available CFD simulation tools are designed for generic purpose. Several of them are suitable and widely used in the building industry. However, the mesh generation process is complicated and time consuming, especially for modeling free form geometric artifacts, e.g., buildings in complex terrains or human bodies in the room. Mesh generation techniques have been well developed in many other fields, such as biomedical engineering (Zhang, Bajaj, and Sohn (2005), Zhang and Bajaj (2006), Zhang, Bajaj, and Xu (2009)), and aerodynamic engineering (Mezentsev (2007), Haimes and Aftosmis (2004)). However, there is relatively little effort to employ mesh generation techniques on applications in architectural engineering. This paper presents the effort to apply quality mesh generation to architectural applications.

A prototype meshing tool has been developed to construct adaptive quadrilateral meshes from two-dimensional image data, e.g., architecture drawings. Based on the type of the elements, two-dimensional meshes fall into three kinds: triangle, quadrilateral, and hybrid meshes. Compared to quad elements, triangles can easily cover irregular shapes in complex domain. However, quadrilateral meshes improve simulation accuracy especially in regions where the gradient of the solution variable is large. For example, in the region of boundary layer flow, orthogonal meshes are highly critical to the solution.

The procedure of the quadrilateral mesh generation is as follows. First the architectural drawing is taken as a two-dimensional image data, which is a sequence of function values greater or smaller than the isovalue representing outside or inside of the simulation domain. The boundary of the building is considered as an isocontour. A starting quad-tree level is selected to preserve the correct topology, and the dual contouring method is used to construct uniform quadrilateral meshes. Then templates are applied to

generate adaptive elements along the boundary. Vertices on the boundary are then projected onto the isocontour, and the pillowing technique is used to generate the boundary layers adjacent to the boundary of the building for the CFD simulations. The thickness of the boundary layer is controlled to achieve the desired y^+ values, according to various requirements of near wall turbulence models. Finally, the whole domain is extended with Cartesian grids to generate coarser meshes with desired element size. The mesh quality is also reported in terms of the shape parameters, the Jacobian, and the condition number of the Jacobian matrix. Furthermore, the skewness angle of the boundary layer elements are reported separately.

After discussing previous works, this paper presents the computation methods and two demonstrations of CFD simulations with meshes generated by the described technique followed conclusions.

PREVIOUS WORKS

Most studies on ventilation performance of the buildings focus on CFD models (Chen (2009)). Flat plat was usually used to represent simple terrains (Chen (2006), Hefny and Ooka (2008)), but the use of CFD to predict the natural ventilation often involves buildings situated in complex terrains. Stangroom (2004) conducted a CFD simulation of the wind field of a cosine shaped hill and the Askervien Hill in Scotland to perform the atmospheric boundary layer simulation in CFX. For the Askervien Hill, points cloud were imported. Curves and surfaces were first reconstructed manually, and then unstructured meshes were generated by CFX-5. A layer of prisms was adopted near the hill boundary to capture the local large gradients of the solution variables.

Understanding the interaction between human body and the ambient thermal environment is one of the major research fields in architectural and building engineering. However in most CFD models, humans are simplified to heated boxes (Zhang et al. (2009), Zhang, Tu, and Ling (2008)), or two connected volumes (Murakami (2000)). Some research studies have shown efforts on numerical geometry reconstruction of human bodies from thermal manikin for CFD simulations (Gao and Niu (2005)). Soensen and Voigt (2003) constructed a surface mesh resembling a seated manikin with the laser scan technique. The model presents currently the best numerical human model for CFD simulation in the building application field. The mesh generation was carried out in the commercial software STAR-CD. The generated meshes consist of 20 layers of prisms extruded from the surface. A large amount of manual interactions were required during the mesh generation process with the currently available mesh generation tools.

The described meshing technique automates the mesh generation process. Starting from 2D architectural drawings, adaptive quadrilateral meshes with boundary layers will be generated automatically. The number of boundary layers and the thickness of each layer can be controlled flexibly to facilitate requirements of different turbulence models and near wall treatments for various simulation scenarios.

COMPUTATIONAL METHODS

1. Data Preparation

The mesh generation algorithm takes the signed distance function data as its input, which can be derived from CAD drawings, points cloud, and images. This paper uses architectural drawings, which are taken as 2D image data. The domain in the CFD simulation is filled with some arbitrary colors to differentiate from the remaining domain. 2D image data is a sequence of function values, $V = \{F(i,j) \mid i,j \text{ are indices in } x,y \text{ coordinates}\}$. Let α be the isovalue, then if $F(i,j) \geq \alpha$, this point is determined to be inside the simulation domain and meshes will be generated accordingly. Otherwise it is considered as outside of the simulation domain and no performance will be conducted. The algorithm presented here is generic, which takes arbitrary 2D images with an isovalue α separating the simulation domain and the non-simulation domain.

2. Mesh Generation

Quadtree/octree-based isocontouring:

The quadtree/octree-based isocontouring method is one of the most robust methods to generate quadrilateral meshes in 2D and hexahedral meshes in 3D for arbitrary shapes with good aspect ratios (Zhang, Bajaj, and Sohn (2005), Zhang and Bajaj (2006), Ju et al. (2002)). Starting with a quadtree level, the isocontouring method will generate one vertex for each cell and result in a uniform quadrilateral mesh. For the cell that intersects the boundary, a minimizer point is calculated by minimizing the quadratic error function (QEF):

$$QEF[x] = \sum (n_i \cdot (x - p_i))^2, \tag{1}$$

where p_i, n_i represent the position and the unit normal vector of the two intersection points respectively. The edges formed by two neighboring minimizer vertices will provide an approximation to the original shape of the boundary.

To further improve the mesh quality, the Laplacian-based smoothing method is used to relocate the vertices on the boundary. The new position is calculated using the middle point of the vertex's two neighbors, which is then projected towards the tangential line along the boundary.

Element decomposition with templates:

Adaptive meshes are generated with further decomposition of the elements along the isocontour using predefined templates without introducing any hanging nodes. The designation of the templates is shown in Fig.1.

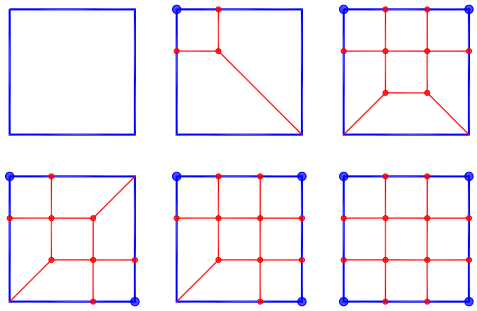

Figure 1: Templates designation for element decomposition. The blue rectangle (bigger rectangle) represents the original quad element. The blue dots (bigger dots) represent vertices on the boundary. The red dots (smaller dots) represent the newly inserted vertices.

Projection:

After templates are applied to the elements along the isocontour, relatively denser meshes are generated near the boundary. As described in the previous section, the original vertices are calculated based on the quadratic error function (Eqn.(1)). Newly inserted vertices are on the edges of the original elements. The vertices can be further moved towards the isocontour in order to achieve a better description of the boundary. The vertices are moved towards the isocontour along the calculated projection directions (Fig.2). The projection direction of the original dual contouring vertex is the average normal directions of the two adjacent edges on the isocontour. The projection direction of the inserted templates vertex is the normal direction of the edges it is inserted into.

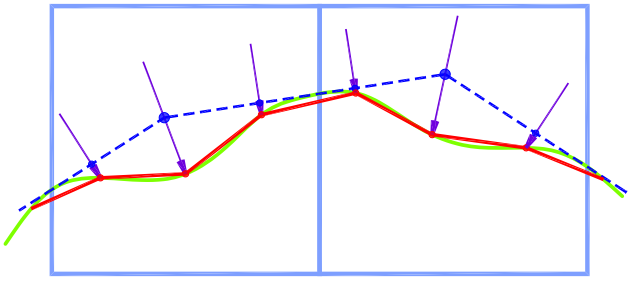

Figure 2: Vertex projection method. The dash lines (blue) dots are the original edges and vertices generated after templates are applied. The arrows are the calculated projection directions. The solid lines (red) and dots are the resulting edges and vertices after projection.

Pillowing:

Thermal and fluid boundary layer exhibits local higher gradient along the normal direction than other directions. A smaller element size along the normal direction is necessary to resolve the solution variables in these regions. Furthermore, it is desirable to have the near-wall meshes orthogonal to the wall. The advancing front method is the most commonly used method for generating boundary layer meshes (Rao (1999), Ito and Nakahashi (2002)). The advancing front method will calculate the surface normal from which the boundary layer mesh grows. The mesh quality is heavily influenced by the deviation of the growth curves from the normal direction to the base triangle (Garimella and Shephard (1998)). Thus, the advancing front method may not perform well for geometry with sharp angles, and special procedures are required to check possible self-intersections of exposed faces.

In this study, the pillowing method (Mitchell and Tautges (1995)) is used to construct boundary layers, starting from the generated quadrilateral meshes. This method can generate layers of elements nearly orthogonal to the boundary, which is the most desired quality for the boundary layer mesh. In addition, the thickness of the newly generated layer of meshes can be controlled by the number of steps and the step size of the smoothing procedure.

The pillowing method is a sheet insertion method. The vertices on the boundary are duplicated and then the corresponding vertices are connected to form a new layer of elements. Then the old vertices on the boundary become interior nodes and all the interior vertices are moved based on a Laplacian smoothing method. The new position of the vertex is the area-weighted average of all its neighboring elements, and the movement of the boundary vertex is restricted along its tangential direction. The smoothing process is an iterative process that the vertex positions are interactively updated. The movements of the vertices are carried out by a series of time steps. In each time step, the vertices move towards the new positions by a step size,

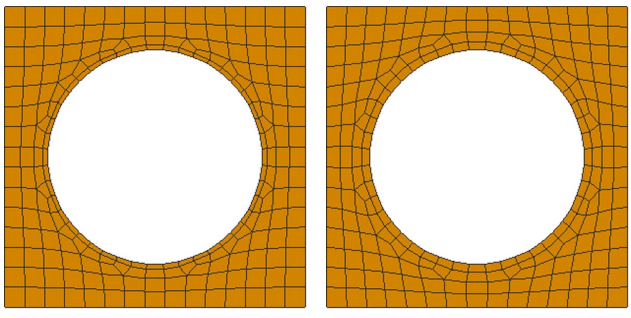

(a) (b)

Figure 3: Boundary layers generated with different number of steps and step sizes. (a) ♯ steps = 500, step size = 0.0004; (b) ♯ steps = 600, step size = 0.001.

and then the area of each element is updated. The thickness of the boundary layer can be controlled by the number of steps and step size, as shown in Fig.3.

Extension:

Based on the meshes generated from the previous step, additional layers are added with the same number of boundary vertices. This method will duplicate the vertices on the domain boundary with the desired number of layers, and locate the new duplicated vertices with the desired element size to add new elements accordingly.

3. Mesh Quality

The shape parameters, the Jacobian and the condition number of the Jacobian matrix are taken as the mesh quality metrics. The shape parameters include the aspect ratio and the skewness angle. There are several ways to define the aspect ratio. In this study the definition from Robinson (1987) is used as shown in Fig.4. First two lines are drawn through the center points of the two opposite sides of the quad. One corresponding square is constructed for each center point line. The aspect ratio of each square is the ratio between its width and length. The aspect ratio of the quad is the smaller aspect ratio of the two squares. The skewness angle is the angle between the two center point lines, the angle α in Fig.4.

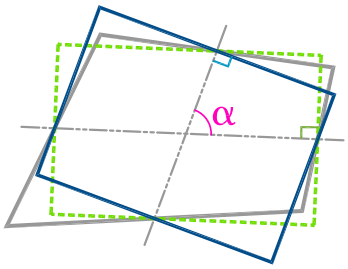

Figure 4: Aspect ratio and skew angle. The two squares are constructed based on the two center point lines (the blue square (solid line) and the green one (dash line)). The aspect ratio of each square is the ratio between its width and length. The aspect ratio of the quad is the larger aspect ratio of the two squares. The skew angle α is the angle between two center point lines.

The Jacobian matrix is the most frequently used mesh quality metric, from which several mesh quality optimization objective functions were derived (Knupp (2000)). Suppose the maximum valence number is M (M $\geq$ 3) for a given mesh, and m_i ($m_i \leq M$) is the valence number of the i^{th} vertex. Let $\{x_j \mid j \leqslant m_i\} \in R^2$ be the set of all the vertices sharing an edge with the i^{th} vertex, and let $\{e_j = x_j - x_i \mid j \leqslant m_i\} \in R^2$ be the set of edge vectors that are connected with the i^{th} vertex. The j^{th} ($j = 1, 2, \ldots, m_i$) Jacobian matrix of the i^{th} vertex is defined as

$$J_j = \begin{bmatrix} e_j & e_{j+1} \end{bmatrix} = \begin{bmatrix} x_j - x_i & x_{j+1} - x_i \\ y_j - y_i & y_{j+1} - y_i \end{bmatrix}. \quad (2)$$

The determinant of the Jacobian matrix is called *Jacobian*, or *scaled Jacobian* if the edge vectors are normalized. The *Jacobian* of a vertex is the minimum value of all its *Jacobians*. An element is called inverted if its *Jacobian* is less than 0. Meshes with *scaled Jacobian=1* are considered to be with good quality.

The condition number of the Jacobian matrix is defined as $\kappa(J) = |J||J^{-1}|$, where $|J^{-1}| = \frac{|J|}{det(J)}$. $|J|$ is the norm of the matrix. Several definitions exist for the matrix norm, however the *Frobenius norm* has been proved to be most effective and most easily implemented in mesh quality metrics (Knupp (2000)), thus is choosen in this study. For a 2×2 matrix, the *Frobenius norm* is $|A|_F = \left(tr\left(A^T A\right)\right)^{1/2}$.

CFD SIMULATIONS

The commercial program FLUENT 6.3 (Fluent (2007)) is used to perform the Computational Fluid Dynamics (CFD) computation. The simulation scenarios include the wind flow field at the ambient environment of a building, and the natural convection around an occupant in the indoor environment.

Flow scenarios in the ambient and indoor space of buildings can be largely divided into high-Reynolds and low-Reynolds flows. The turbulent flow is significantly affected by the presence of walls. Being constrained to the no-slip condition, the velocity at the wall surface has to be zero, and the shear stress reaches to the maximum. Given the near-wall region complication, treatments of the two kinds of flows are different. Experiments have shown that the near-wall region can be subdivided into three layers as shown in Fig.5. The distance of each layer from the boundary is expressed in terms of a non-dimensional value y^+, which is defined as $\frac{\rho u_\tau y}{\mu}$ (Chung (2002)). There are three sublayers in the near wall flow field.

- Viscous sublayer: nearly laminar flow region;
- Buffer layer (blending region): the transition region between the viscous laminar flow to the fully developed turbulent flow. The effects of molecular viscosity and turbulence are equally important;
- Fully turbulent layer (Log-Law layer): fully developed turbulent flow, where turbulence is the dominating term.

Most high-Reynolds-number turbulence models are primarily valid for the main stream of the flow field. Near-wall effects require additions or modifications to the basic

Table 1: Mesh quality summary of generated meshes.

Meshes	Aspect Ratio (avg, stdDev, max, min)	Skewness Angle (avg, stdDev, max, min)	Scaled Jacobian (avg, stdDev, max, min)	Condition Number (avg, stdDev, max, min)
Reichstag Building	(0.65, 0.03, 1.00, 0.02) 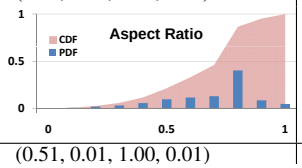	(89.18, 5.46, 150.03, 26.23) 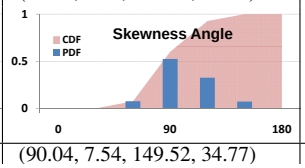	(0.91, 0.01, 1.00, 0.21) 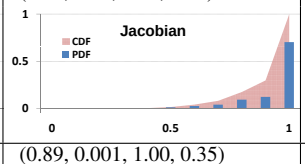	(1.12, 0.05, 4.67, 1.00) 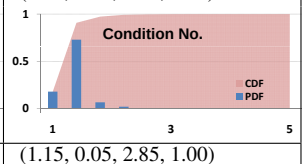
Lady Mona Lisa	(0.51, 0.01, 1.00, 0.01) 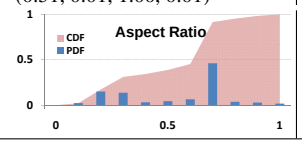	(90.04, 7.54, 149.52, 34.77) 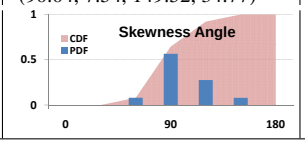	(0.89, 0.001, 1.00, 0.35) 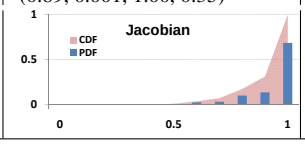	(1.15, 0.05, 2.85, 1.00) 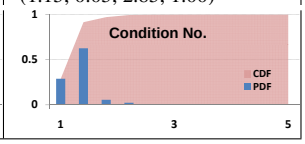

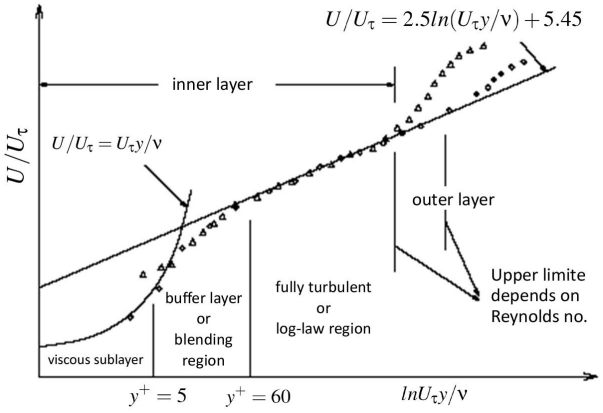

Figure 5: The three sublayers of the flow field of the near wall region in semi-log plot (Fluent (2007)).

model (Pope (2000)), thus "wall-functions" have been developed for the turbulence models. The "wall-functions" approximate the near wall-region, in which solution variables change most rapidly.

While in the case of low-Reynolds-number flow fields and high pressure gradient flows, such as the buoyancy flow, the "wall-functions" approach is less appropriate since the hypotheses underlying the wall functions are less valid. In such cases, the "wall-model" approach with sufficient mesh resolution is recommended.

The requirements for the resolutions of near wall meshes in different approaches are:

- For standard "wall-functions" under high-Reynolds-number turbulence models, the near wall element centroid should be in the log-law layer $30 < y^+ < 300$. A y^+ value close to 30 is most desirable;
- The mesh should avoid the buffer layer ($y^+ = 5 \sim 30$) as much as possible;
- For "wall-model" approaches, the value of y^+ should be in the order of 1. The y^+ value inside the viscous sublayer satisfying $y^+ < 3 \sim 5$ is acceptable.

The "wall-functions" approach for high-Reynolds-number turbulence models and the "wall-model" approach for the low-Reynolds-number flow are demonstrated in this paper. The mesh generation requirements and the resulting y^+ values are presented in detail as follows.

NUMERICAL RESULTS

The mesh generation algorithm is applied to two demonstrative examples, the wind flow field around Reichstag Building at the outdoor ambient environment, and the natural convection around Lady Mona Lisa in the indoor environment The mesh quality metrics of the generated meshes are listed in Table 1. The orthogonality of the boundary layer mesh is crucial for the boundary layer flow simulation. The skewness angles of the boundary layer elements are reported separately in Table 2. As shown in the table, the average skewness angle is around 89° for the two sets of generated meshes, with the standard deviation around 18°. Furthermore, on average of the two sets of meshes, more than 60% of all the elements have the skewness angle within $90° \pm 10°$, and more than 50% within $90° \pm 5°$.

Table 2: Statistics on the skewness angle of the generated boundary layer meshes.

Meshes	Skewness Angle (avg, stdDev, max, min)
Reichstag Building	(88.70, 18.86, 147.31, 26.86) 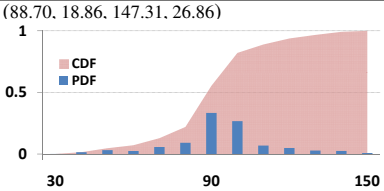
Lady Mona Lisa	(89.60, 18.88, 145.24, 32.42) 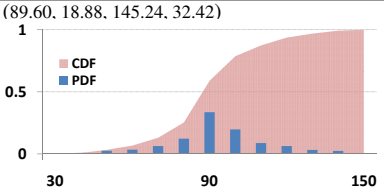

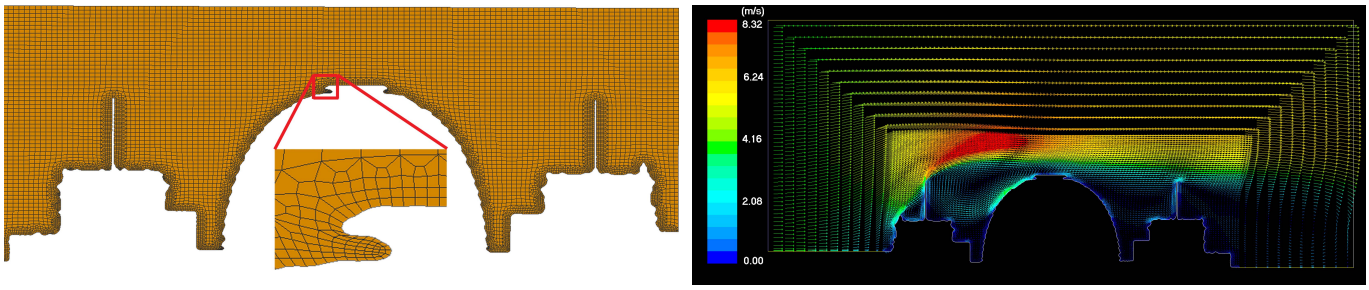

(a) (b)

Figure 6: The wind flow field at the ambient of the Reichstag Building (high-Reynolds-number flow). (a) The constructed all quadrilateral mesh; (b) The resulting velocity vector field of the flow.

1. The High-Reynolds-Number Flow Field at the Ambient of Reichstag Building

The Reichstag Building designed by Sir Norman Foster is selected for the simulation of flow field at the building ambient. The generated meshes are shown in Fig.6(a) and the quality parameters are listed in Table 1 and Table 2.

The boundary conditions are set as follows: wind comes from the left hand side at a velocity of 4 m/s, the right hand side boundary is set as the out flow, the top and the bottom boundaries are symmetric. The standard $k-\varepsilon$ model is chosen as the turbulence model, with a turbulent intensity of 20%, a turbulent length scale of 1m, and standard wall functions applied. The requirement of near wall meshes is $30 < y^+ < 300$. The solution dependent variable y^+ ($y^+ = \frac{\rho u_\tau y}{\mu}$) is first calculated using the non-dimensional analysis method. The reference velocity is the incoming wind velocity of 4 m/s, the air viscosity μ is 1.79×10^{-5} $kg/m{\cdot}s$, and the air density at $310K$ is 1.138 kg/m^3. In order to get $y^+ \sim 30$, the thickness of the first layer needs to be 4.72×10^{-4} m. As stated earlier, the boundary layer thickness can be controlled by the step size and the number of steps in the smoothing procedure. Two boundary layers are generated. The step size and the number of steps are (600, 0.01) for both the first layer and the second layer. Generated mesh and the flow field are shown in Fig.6. The resulting y^+ values are shown in Fig.7.

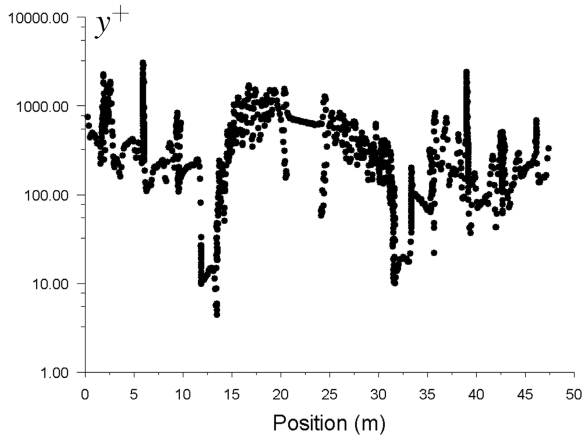

Figure 7: The plot of the y^+ values of the first layer near the boundary of the Reichstag Building. The resulting y^+ values are 85 elements (6.9%) with $y^+ < 30$, 525 elements (43%) with $30 < y^+ < 300$, 618 elements (50%) with $y^+ > 300$.

2. The Low-Reynolds-Number Flow Field of the Natural Convection around a Human Body

The simulation of the pure natural convection scenarios around a human body in an enclosed space is conducted. The portrait of Lady Mona Lisa in Gioconda is chosen. The boundary conditions of the natural convection simulation are as follows: the human body is at constant temperature of 310K, the top boundary is a cool surface at a constant temperature of 300K, the left and right boundaries are symmetric.

As stated in the previous section, natural convection is a typical low-Reynolds-number flow. Therefore, the standard $k-\omega$ is chosen, which incorporates modifications for low-Reynolds-number effects on fine meshes (Fluent (2007), Pope (2000)). The requirement on the first layer of meshes is $y^+ < 3 \sim 5$. To achieve the desired y^+ value, the thickness of the boundary layer is calculated using the non-dimensional analysis method. The model for natural convection along a two-dimensional infinite vertical flat plate is used to calculate the reference velocity of the buoyancy induced flow field. The governing equations for natural convection along a infinite vertical flat plate are:

$$\frac{\partial u}{\partial x}+\frac{\partial v}{\partial y}=0, \tag{3}$$

$$u\frac{\partial u}{\partial x}+v\frac{\partial u}{\partial y}=\beta(T-T_\infty)_g+\gamma\frac{\partial^2 u}{\partial^2 y}, \tag{4}$$

$$\rho C_p\left(u\frac{\partial T}{\partial x}+v\frac{\partial T}{\partial y}\right)=k\frac{\partial^2 T}{\partial^2 y}. \tag{5}$$

In the $x-momentum$ equation (Eqn.(4)), assume $v=0$ and neglect the viscosity term, then the equation is reduced to ${u_{max}}^2(x) \sim 2\beta(T-T_\infty)gx$. As shown in Fig.9, the maximum velocity of the buoyancy flow along the infinit flat plate is a function of height x. The simulation

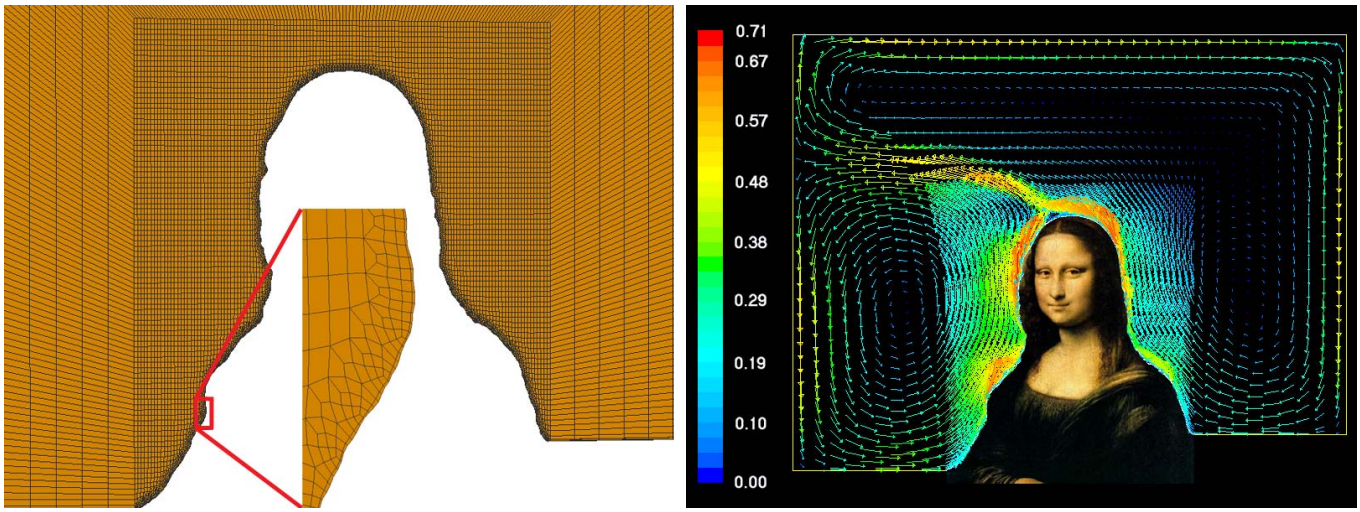

(a) (b)

Figure 8: The natural convection around an occupant (Lady Mona Lisa) in the indoor environment (low-Reynolds-number flow). (a) The constructed all quadrilateral mesh; (b) The resulting natural convection velocity field.

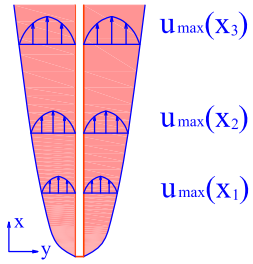

Figure 9: The natural convection along an infinite flat plat. The maximum velocity of the buoyancy flow along the infinit flat plate is the function of height x.

condition is at the room temperature range, thus air density of $1.138kg/m^3$ at $313K$ ($40°C$) and $1.184kg/m^3$ at $298K$ ($25°C$) is used to calculate the thermal expansion coefficient which is $\beta = 3.37 \times 10^{-5}/K$. The constant of gravity acceleration is $g = 9.8m/s^2$. The resulting maximum velocity u_{max} at $x = 1$ is $u_{max}(1) = 0.81\ m/s$. To achieve a y^+ value of less than 3 ($y^+ = \frac{\rho u_\tau y}{\mu}$), the maximum element size of the first layer should be 3.83×10^{-5} m. The step size and the number of steps for the first and the second layers are (0.001, 500) and (0.01, 800), respectively. Fig.8 shows the generated quadrilateral meshes as well as the resulting velocity field of the natural convection flow field. The resulting y^+ plot of the first layer is shown in Fig.10.

CONCLUSION

This paper presents a prototype automatic mesh generation tool to generate adaptive quadrilateral meshes from architecture drawings for CFD simulations. Starting from 2D image data, adaptive quadrilateral meshes are constructed automatically. The nearly orthogonal boundary layer is generated and the thickness is controlled to facilitate various simulation scenarios. The generated meshes have shown good quality in terms of shape parameters, the Scaled Jacobian, and the condition number of the Jacobian matrix. The skewness angle of the boundary layer is reported as well. More than 60% of the elements have the skewness angle within $90° \pm 10°$, and more than 50% elements have the skewness angle within $90° \pm 5°$.

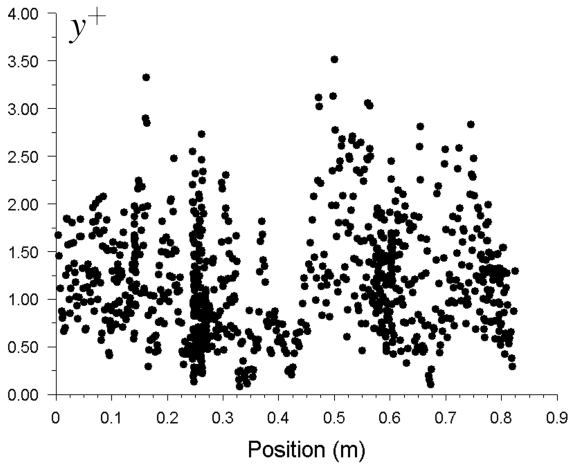

Figure 10: The plot of the y^+ values of the first layer near the boundary of the lady. The majority falls under 3, which is the most desirable boundary layer mesh quality for the buoyancy driven flow.

The work presented here is part of the on-going research on mesh generation tool for applications in architecture. Future work includes the following:

- Develop 3D mesh generation tool for architecture applications, supporting the extraction of geometry

models from IFC (Industry Foundation Class) files.

- Develop algorithms to detect different surface characteristics in architecture applications for boundary condition setting in CFD simulations.

- Compare the CFD simulation results with experimental data, and investigate ways to improve the simulation accuracy via mesh generation.

REFERENCES

Chen, Q. 2006. "Sustainable Urban Housing in China Principles and Case Studies for Low-Energy Design." In *Paradigm Gems 2*, edited by L. Glicksman and J. Lin, 116–123. Springer Netherlands.

Chen, Q.. 2009. "Ventilation Performance Prediction for Buildings: A Method Overview and Recent Applications." *Building and Environment* 44 (4): 848 – 858.

Chung, T. J. 2002, January. *Computational Fluid Dynamics*. Cambridge University Press.

Fluent. 2007. *FLUENT 6.3 Documentaion*.

Gao, N. P., and J. L. Niu. 2005. "CFD Study of the Thermal Environment around a Human Body: A Review." *Indoor and Built Environment* 14 (1): 5–16.

Garimella, R., and M. Shephard. 1998. "Boundary Layer Meshing for Viscous Flows in Complex Domain." *Proceedings of 7th Internaltional Meshing Roundtable*, pp. 107–118.

Haimes, R., and M. J. Aftosmis. 2004. "Watertight Anisotropic Surface Meshing Using Quadrilateral." *Proceedings of 4th International Meshing Roundtable*, pp. 311–322.

Hefny, M. M., and R. O. Ooka. 2008. "Influence of Cell Geometry and Mesh Resolution on Large Eddy Simulation Predictions of Flow Around a Single Building." *Building Simulation* 1 (3): 251–260.

Ito, Y., and K. Nakahashi. 2002. "Unsructed Mesh Generation Algorithms for Viscous Flow Computations." *Proceedings of 11th International Meshing Roundtable*, pp. 367–377.

Ju, T., F. Losasso, S. Schaefer, and J. Warren. 2002. "Dual Countouring of Hermite Data." *Proceedings of SIGGRAPH*, pp. 339–346.

Knupp, P. M. 2000. "Achieving Finite Element Mesh Quality Via Optimization of the Jacobian Matrix Norm and Associated Quantities, Part I-A Framework for Surface Mesh Optimization." *International Journal for Numberical Methods in Engineering*, no. 48:401–420.

Mezentsev, A. 2007. "An Efficient Geometrical Model for Meshing Applications in Heterogeneous Environment." *Proceedings of 4th International Meshing Roundtable*, pp. 150–168.

Mitchell, S., and T. Tautges. 1995. "Pillowing Doublets: Refining a Mesh to Ensure that Faces Share at Most One Edge." *Proceedings of 4th International Meshing Roundtable*, pp. 231–240.

Murakami, S. 2000. "Combined Simulation of Airflow, Radiation and Moisture Transport for Heat Release from a Human Body." *Building and Environment* 35:489–500(12).

Pope, S. B. 2000. *Turbulent Flows*. Cambridge: Cambridge University Press.

Rao, D. W. 1999. "Anisotropic Tetrahedral Mesh Generation." Ph.D. diss., Rensselaer Polytechnic Institute.

Robinson, J. 1987. "CRE Method of Element Testing and the Jacobian Shape Parameters." *Engineering Computations*, no. 4:113–118.

Soensen, D. N., and L. K. Voigt. 2003. "Modelling Flow and Heat Transfer around a Seated Human Body by Computational Fluid Dynamics." *Building and Environment* 38 (6): 753 – 762.

Stangroom, P. 2004. "CFD Modelling of Wind Flow Over Terrain." Ph.D. diss., University of Nottingham.

Zhang, R., G. Tu, and J. Ling. 2008. "Study on Biological Contaminant Control Strategies Under Different Ventilation Models in Hospital Operating Room." *Building and Environment* 43 (5): 85–94.

Zhang, Y., and C. Bajaj. 2006. "Adaptive and Quality Quadrilateral/Hexahedral Meshing from Volumetric Data." *Computer Methods in Applied Mechanics and Engineering* 9 (195): 942–960.

Zhang, Y., C. Bajaj, and B-S. Sohn. 2005. "3D Finite Element Meshing from Imaging Data." *The special issue of Computer Methods in Applied Mechanics and Engineering (CMAME) on Unstructured Mesh Generation* 48 (194): 5083–5106.

Zhang, Y., C. Bajaj, and G. Xu. 2009. "Surface Smoothing and Quality Improvement of Quadrilateral/Hexahedral Meshes using Geometric Flow." *Communications in Numerical Methods in Engineering* 25 (1): 1–18.

Zhang, Z., X. Chen, S. Mazumdar, T. Zhang, and Q. Chen. 2009. "Experimental and Numerical Investigation of Airflow and Contaminant Transport in An Airline Cabin Mockup." *Building and Environment* 44 (1): 85–94.